

A Model for Multi-Agent Heterogeneous Interaction Problems

Christopher D. Hsu^{1,2}, Mulugeta A. Haile¹, and Pratik Chaudhari²

Abstract—We introduce a model for multi-agent interaction problems to understand how a heterogeneous team of agents should organize its resources to tackle a heterogeneous team of attackers. This model is inspired by how the human immune system tackles a diverse set of pathogens. The key property of this model is “cross-reactivity” which enables a particular defender type to respond strongly to some attackers but weakly to a few different types of attackers. Due to this, the optimal defender distribution that minimizes the harm incurred by attackers is supported on a discrete set. This allows the defender team to allocate resources to a few types and yet tackle a large number of attacker types. We study this model in different settings to characterize a set of guiding principles for control problems with heterogeneous teams of agents, e.g., sensitivity of the harm to sub-optimal defender distributions, teams consisting of a small number of attackers and defenders, estimating and tackling an evolving attacker distribution, and competition between defenders that gives near-optimal behavior using decentralized computation of the control. We also compare this model with reinforcement-learned policies for the defender team.

I. INTRODUCTION

Consider the adaptive immune system which protects an organism from pathogens [1]. Some pathogens are persistent but benign (e.g., common cold) and others are rare but dangerous (e.g., HIV). There is a vast number ($\sim 10^{30}$) of other pathogens on this spectrum. Tackling every pathogen optimally requires a specialized receptor (these are proteins expressed by lymphocytes whose molecules bind to the molecular constitution of pathogens). It would intuitively seem that to minimize harm, the distribution of receptors should be identical to the distribution of pathogens in the environment. The immune system instead allocates a relatively larger amount of resources to tackling pathogens that cause large harm even if they are rare, and relatively fewer resources to pathogens which cause less harm, even if they are encountered frequently. This allocation strategy might seem counter-intuitive, but there are two underlying principles. First, a constraint on the metabolic energy spent on maintaining a large receptor repertoire limits the total number of diverse receptors. And second, there exist specialized receptors that detect and tackle a specific pathogen with high probability, but these same receptors can also respond to other pathogens with a smaller probability.

The above two principles allow the immune system to minimize harm more effectively than if it were to special-

ize a receptor for each pathogen. Multi-agent interaction problems, where a team of defenders interacts with a team of attackers, could benefit from similar principles.

Fig. 1 shows a hypothetical scenario where the distribution of attackers and defenders are illustrated for electronic, ground, and air systems. Teams can consist of a heterogeneous group of agents with different capabilities, say offensive or defensive skills, sensing modalities, operating environments, and/or mobility. The goal of this paper is to understand how defenders can (a) organize a team to minimize the harm caused by different types of attackers, and (b) interact and recognize the types and capabilities of the attackers in order to adapt the defender types to evolving attacker types.

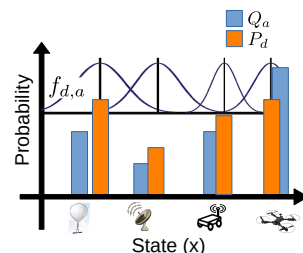


Fig. 1: Orange defenders from distribution P_d interact with blue attackers from distribution Q_a with probability $f_{d,a}$.

A. Contributions

We use a theoretical model of the human adaptive immune system [1] to understand how a defending team can optimally allocate its resources to minimize the harm incurred from a heterogeneous team of attackers. We focus our analysis on two situations: (i) when no single defender can defend against every type of attacker, and (ii) when defenders have limited resources that they should devote optimally to tackle attackers.

We develop a technique to estimate and adapt to an unknown and evolving heterogeneous attacker distribution. When defenders do not have full knowledge of the attacker distribution, we show how to use the information from encounters between defender-attacker agents to estimate the attacker distribution and adapt the defender distribution accordingly. We consider two situations: (i) when the attacker distribution is stationary and does not change over time, and (ii) when it evolves over time.

We show that defenders can achieve near-optimal harm when defender agents compete with each other for successful encounters with attacking agents. Centralized computation may seem necessary to select the optimal defender distribution because it depends upon both local and global structure of the attacker distribution. We study the “centralized estimation and decentralized control” setting where information obtained from individual interactions with the attackers is shared with all the defenders but different

¹DEVCOM Army Research Laboratory christopher.d.hsu.civ@army.mil, mulugeta.a.haile.civ@army.mil

²Department of Electrical & Systems Engineering and the GRASP Laboratory at the University of Pennsylvania. chs8@seas.upenn.edu, pratikac@seas.upenn.edu

defenders use this information in different ways, e.g., deciding which attacker type to tackle. The induced competition between defenders and successful interactions with attackers acts as a reward to encourage the congregation of specific defender types. We show how such local computation leads to near-optimal defender distributions, both with the use of competition dynamics and reinforcement learning.

II. RELATED WORK

Interactive multi-agent problems, e.g., pursuit-evasion games, have seen a wide range of perspectives [2, 3], surveys [4, 5], and applications such as search and rescue [6] and environmental monitoring [7]. Problems with multiple agents are complex due to their high dimensional state-space [8]. A theme that has emerged recently in reinforcement learning-based multi-agent control [9, 10] is to obtain decentralized, cooperative policies [11] for non-stationary problems with limited information. A popular paradigm is to train a centralized policy and execute it in a decentralized fashion [12]. Emergence of coordination has also been studied [13]. These methods typically suffer from poor sample complexity but some works have scaled them to large problems [14], including problems with up to 1000 attackers and defenders using heuristics [15]. There are also a number of works that use bio-inspired approaches mimicking the behavior of ants, bees and flocks [16, 17] for multi-agent control.

In the context of the above literature, the place of the present paper is to study a theoretical model where large heterogeneous multi-agent interaction problems can be analyzed precisely. This model has several benefits, e.g., using the model, we can estimate and adapt to an unknown attacker distribution and find that even if the defenders do not accurately estimate the attacker distribution, the eventual harm can be near-optimal. This model also establishes guiding principles for building multi-agent control policies, e.g., inducing competition among the defender agents for successful encounters can lead to near-optimal harm. Finally, we can simulate the model even when the number of defenders and attackers is extremely large. A large number of papers, including many above, have sought to understand trends in learned policies and costs for multi-agent systems using simulations. The utility of our model is that it is a more straightforward approach to achieving the same insights.

Modeling heterogeneity, which is the focus of this paper, has received relatively little interest [18]. Heterogeneity comes in many forms such as differences in roles [19], robotic capabilities and or sensors [20, 21], dynamics [22, 23], and even teams of air and ground robots [24, 25]. But algorithmic methods that can tackle large-scale heterogeneity have been difficult to build. A taxonomy for heterogeneous multi-robot systems in introduced [26] and a method for more explicit handling of the heterogeneous systems is developed for RL. Task assignment with heterogeneous agents [27] is another similar problem to ours, but a desired trait distribution is necessitated by the objective instead of calculating it explicitly.

In comparison, the present paper uses a simple formulation to understand what distribution is the best and how to devote heterogeneous agents optimally in a multi-agent interaction problem.

III. PROBLEM FORMULATION

Let Q_a be the probability that denotes the next attack will be caused by an attacker of type a . Let P_d be the probability of a defender of type d being present. We wish to compute the optimal distribution of the defenders P_d^* that minimizes the harm caused by this infestation before full recognition of the entire repertoire of attackers. In biology, attackers a and defenders d interact in an abstract metric space called the shape-space [28]. For the purposes of this paper, we should think of the shape space as the real-valued space of the different types of agents; if attacker types a, a' are similar to each other then $|a - a'|$ is small.

a) Interaction between attackers and defenders: Let $f_{d,a}$ denote the probability that defender d interacts with an attacker a successfully; we will call this probability “cross-reactivity” and such a successful interaction “recognition”. Let us assume that cross-reactivity is a Gaussian $f_{d,a} \propto \exp\left(-\frac{(d-a)^2}{2\sigma^2}\right)$ where σ denotes the bandwidth. Defenders d that have a low probability under this probability distribution have a small chance of recognizing an attacker a . The total probability of recognizing an attacker a is $\hat{P}_a = \sum_d f_{d,a} P_d$. We will call this the “coverage”. Naively, the defender team would allocate resources to simply maximize coverage.

We model the interaction between an attacker a and a defender d as a Poisson random variable with rate $\lambda_a(t)$. Larger the number of attackers, larger the rate of interaction with them. We model this as a rate that increases exponentially with time, i.e., $\dot{\lambda}_a(t) = \lambda_a \nu'_a$ starting from some initial rate $\lambda_a(0) = 1$. In biology, the rate of interaction with a particular type of pathogen increases because the number of individuals of that pathogen grows with time (if the immune system does not recognize it). For our problem, the number of attackers could grow because an attacker, e.g., a particular type of adversary, reinforces its position by producing more agents of its type. Under this assumption, the expected number of interactions of an attacker a with some defender is $m_a(t) = \int_0^t d\tau \lambda_a(\tau) \approx \lambda_a(0)(e^{\nu'_a t} - 1)/\nu'_a$.

b) Harm caused by an attacker: We denote the number of attackers of type a by $m_a(t)$. This also grows exponentially $\dot{m}_a(t) = m_a \nu_a$ starting from some $m_a(0) = 1$ until the time this attacker is recognized. Exponents ν_a and ν'_a may be different because the number of attackers a that cause harm may grow differently than the number of attackers a that can be observed by the defense. Let us assume that unsuccessful interactions of defenders with attackers cause one unit of harm. For large times $t \approx \log(m_a/\lambda_a(0))/\nu'_a$, the expected harm caused by an attacker of type a after m unsuccessful interactions is

$$F_a(m) = F_a(0) \left(\frac{m}{\lambda_a(0)} \right)^{\nu_a/\nu'_a} \propto m^\alpha; \quad (1)$$

where $\alpha = \nu_a/\nu'_a$. Observe that in this case, $F_a(m)$ is polynomial in the number of interactions m in this paper, but it can also take other forms, e.g., $F_a(m) = 1 - e^{-\beta m}$ would model the situation where the harm plateaus after a large number of interactions. The harm \bar{F}_a caused by an attacker a until it is recognized by the defenders is thus

$$\bar{F}_a(P_d) = \tilde{P}_a \int_0^\infty dm F_a(m) e^{-m\tilde{P}_a}. \quad (2)$$

We call this the ‘‘empirical harm’’ because we will be able to estimate it by simulating interactions between attackers a sampled from Q_a and defenders d sampled from P_d . The harm \bar{F}_a is a function of the defender distribution P_d through the coverage \tilde{P}_a .

c) *Minimizing the harm*: The harm caused by attackers sampled from Q_a is

$$\text{Harm}(P_d) = \sum_a Q_a \bar{F}_a. \quad (3)$$

It is a function of the defender distribution P_d and our goal is to minimize it. When $F_a(m) = m^\alpha$, this optimization problem can be solved analytically to obtain

$$\bar{F}_a = \Gamma(1 + \alpha) / \tilde{P}_a^\alpha, \quad (4)$$

where Γ is the Gamma function. We will refer to this as the ‘‘analytical harm’’ in the rest of the paper. The harm incurred for different settings, e.g., a sub-optimal defender distribution P_d , a reinforcement learned-policy, etc. can all be compared to this quantity.

Q_a	Probability of attacker of type a (attacker distribution)
P_d	Probability of defender of type d (defender distribution)
$f_{d,a}$	Probability of recognition of type a by type d (cross-reactivity)
\bar{F}_a	Harm from attacker a
N_a	Number of attackers of type a (used for simulation)
N_d	Number of defenders of type d (used for simulation)

TABLE I: To help the reader keep track, we collect the most important quantities of this model in one place.

IV. OPTIMAL DEFENDER DISTRIBUTION IS SUPPORTED ON A DISCRETE SET

For a Gaussian $Q_a \propto e^{-a^2/(2\sigma_Q^2)}$, it can be shown [1] that when σ is smaller than a threshold $\sigma_Q\sqrt{1+\alpha}$, the optimal defender distribution is also Gaussian

$$P_d^* \propto e^{-\frac{d^2}{2((1+\alpha)\sigma_Q^2 - \sigma^2)}}.$$

Note that the variance is negative if $\sigma/\sigma_Q > \sqrt{1+\alpha}$. So if the bandwidth is above this threshold, the optimal defense is a Dirac delta at the origin. This shows that cross-reactivity allows concentrated distributions and reduces the need to maintain a diverse number of defenders. We can also show this mathematically where we can turn the variational problem in (3) into a standard optimization problem by assuming a parametric form for the defender distribution $P_d = e^{-d^2/(2\sigma_P^2)}$ (by symmetry it has to be centered at $d = 0$). For a Gaussian Q_a , we can now minimize the harm in (3), to see that the solution has $\sigma_P = 0$.

This short calculation is a key result of our paper. In biology, cross-reactivity allows a receptor to bind to different pathogens to varying degrees; a non-zero bandwidth σ thus reduces

the number of different types of defenders that it needs to maintain. It suggests that for multi-agent interaction problems, the optimal defender distribution could be supported on a specific set of defender types and need not span the entire spectrum of the attacker types.

Roughly speaking, a defender distribution P_d^* supported on a discrete set allows capturing large parts of the attacker distribution Q_a with few resources (defender types) due to cross-reactivity $f_{d,a}$. Larger the cross-reactivity bandwidth σ , more the spacing between the atoms of P_d^* . Although, we have argued for discreteness when Q_a is Gaussian above (this the simulation in Fig. 2) this result is expected to hold in general; see the numerical simulation in Fig. 3. Let us note that such discrete solutions are seen in many other problems, e.g., capacity of a Gaussian channel under an amplitude constraint [29], discrete priors in Bayesian statistics [30], etc.

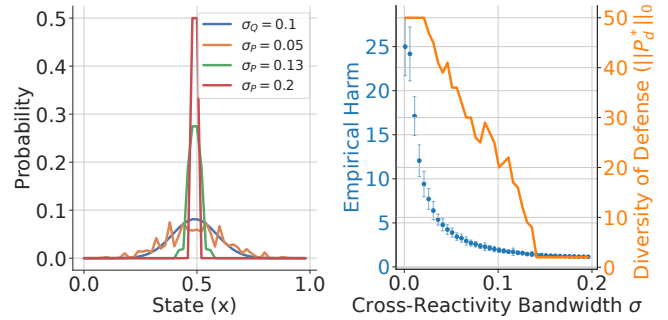


Fig. 2: A simulation of $\sum_a N_a = 100$ attackers sampled from a Gaussian Q_a with $\sigma_Q = 0.1$ interacts with $\sum_d N_d = 100$ defenders sampled from P_d^* for different values of σ_P . **Left:** For $\alpha = 1$, when $\sigma_P \geq \sigma_Q\sqrt{2}$ the optimal P_d^* which is a Gaussian tends towards a Dirac delta distribution at the origin. **Right:** In the simulation, as we increase σ_P beyond $\sigma_Q\sqrt{2}$, the empirical harm, i.e., the average unsuccessful interactions until all attackers are recognized, decreases (blue). The number of distinct defender types also decreases (orange).

A. The multi-agent heterogeneous interaction problem

Let us now consider a non-Gaussian attacker distribution. We drew samples from a log-normal distribution with coefficient of variation $\kappa^2 = \exp(\sigma_Q^2) - 1$ where $\kappa = 5$ and recorded the probabilities of these samples under the log-normal. Our attacker distribution Q_a is supported only on these samples with probabilities of each attacker given by the corresponding probabilities under the log-normal distribution. We numerically optimized (3) to compute the optimal defender distribution P_d^* for this attacker distribution Q_a ; this allows us to calculate the analytical harm (4). We next simulated a 1000 multi-agent interaction problems with 100 attackers sampled from Q_a and 100 defenders sampled from different distributions P_d (including P_d^*) to understand how the empirical and analytical harm change. Attackers proliferated at rate $\nu_a = 1$ and the rate of interactions with them increased at rate $\nu'_a = 1$.

Fig. 3 (left) shows the attacker distribution Q_a (blue), the optimal defender distribution P_d^* (orange) and the harm

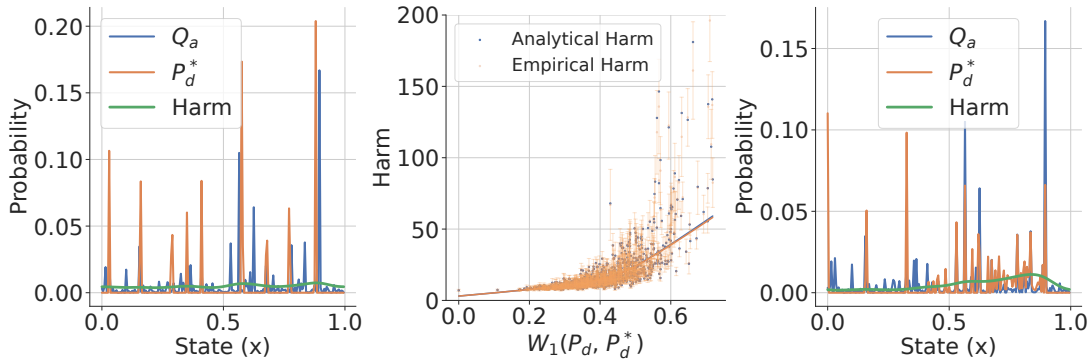


Fig. 3: Left: Simulation of the interaction of defenders (orange) with attackers from distribution Q_a (blue). The optimal defender distribution P_d^* (orange) is found by optimizing (3). Cross-reactivity $f_{d,a}$ with bandwidth $\sigma = 0.05$ leads to a discrete distribution. The harm $Q_a \bar{F}_a$ caused by attackers of different types (green) is uniform across the domain. **Middle:** The harm incurred using a non-optimal P_d increases as the difference measured by the Wasserstein distance between the probability P_d and probability P_d^* increases. To obtain this plot, we sampled 1000 different P_d s (by perturbing the optimal P_d^* using log-normal noise) and computed the empirical and analytical harm against a fixed Q_a . This experiment also indicates that the analytical harm (4) is close to the mean of the empirical harm over 100 episodes of our experiments using (2) for a broad regime. **Right:** Defenders (orange) with cross reactivity bandwidths $\sigma \in \{0.05, 0.01, 0.001\}$, (large to small bandwidth from left to right) for the domain $\in [0, 1]$ split into thirds, interact with attackers from a distribution Q_a (blue) The harm caused by attackers ($Q_a \bar{F}_a$) on the left (when $\sigma = 0.05$) is small compared to the right third with $\sigma = 0.001$.

incurred (green). As expected from our discussion in the previous section, the defender distribution obtained from numerical optimization of (3) seems to be supported on a discrete set. These atoms are close to the atoms of Q_a with similar probabilities, although they do not match exactly. Note that the cross-reactivity $f_{d,a}$ allows defender types to be slightly different than attacker types and yet recognize them successfully. The harm incurred $Q_a \bar{F}_a$ by attackers of different types (in green) is relatively constant across the domain in spite of the discrete-like distribution of the defender distribution. This is a key property of our model. It can be used as a desideratum, or also an evaluation metric, for multi-agent control policies obtained by different methods such as reinforcement learning (see §VIII).

Fig. 3 (middle) shows the analytical and empirical harm for sub-optimal P_d . We will use the 1-Wasserstein metric [31] to measure distances between different defender distributions. This is reasonable because from the previous paragraph, we expect that two distributions P_d with atoms close to each other may incur similar harm, even if the atoms are not exactly the same. The 1-Wasserstein metric for probability distributions on one-dimensional domains is

$$W_1(P_d, P_d^*) = \int_0^1 |F_{P_d}(x) - F_{P_d^*}(x)| dx,$$

where $F_P(x) = \int_0^x P(y) dy$ is the cumulative distribution function; in our simulations we use a discretization of our shape-space $x \in [0, 1]$ and can calculate this integral easily. Our simulation results are validated by the fact that the empirical harm closely tracks the analytical harm in Fig. 3 (middle). Furthermore, it is noticeable that the variance of the empirical harm across multiple simulations increases as P_d becomes more sub-optimal. This is not directly implied by (4) (which only optimizes the average harm). But it is intuitive: as P_d becomes more sub-optimal, the absence of certain defender types in the team leads to proliferation of

certain attacker types, until the small cross-reactivity $f_{d,a}$ from some far away defender type manages to recognize the proliferated attacker type. Our model therefore suggests that if the defender team does not have enough resources (defender types) to build the optimal P_d , one should not only minimize the expected harm (as is typically done in multi-agent control objectives) but also the variance of the harm.

Fig. 3 (right) studies the harm for an attacker distribution Q_a (blue) drawn from a log-normal distribution with $\kappa = 5$ for the situation when each defender can have a different cross-reactivity bandwidth (e.g., a flying platform can tackle many different types attackers while a ground robot can tackle fewer types). We created defenders with three different bandwidths $\sigma \in \{0.05, 0.01, 0.001\}$ (large bandwidths to the left of the domain and small ones to the right). Note that P_d^* depends on σ and therefore the optimal defender distributions for the bandwidths are different. While we do not know the solution of (3) in closed-form like (4) for the case when different defenders have different cross-reactivity, we can numerically optimize (3) to compute P_d^* . As the figure shows, the harm (green) caused by attackers of different types is smaller for defenders types have large bandwidths in the left-hand-side of the domain and higher towards the right.

V. LIMITED NUMBER OF DEFENDERS IN THE REPERTOIRE

The analytical harm in (4) is a population-level estimate, i.e., it is valid for an infinite number of attackers and defenders. We will next study the problem when the number of attackers and defenders is finite with the goal of understanding the regime under which this population-level model holds.

Each attacker, out of N_a possible attackers of type a , interacts with each defender, out of N_d defenders of type d , at each iteration. A recognition event occurs with cross-reactivity probability $f_{d,a}$ and if none of the defenders recognize the

attacker, then 1 unit of harm is incurred from each attacker. If one of these interactions is successful, then we set number of attackers of that type to zero. Fig. 4 (left) shows the empirical and analytical harm (calculated using (4)) when $\sum_a N_a = \sum_d N_d$, i.e., when the number of attackers is equal to the number of defenders (they are distributed according to their irrespective distributions Q_a and P_d). Empirical harm has a larger variance when the number of agents is small, but it is remarkable that our model allows us to estimate this variance accurately. In Fig. 4 (right), we sweep over both the number of attackers $\sum_d N_a$ and the number of defenders $\sum_d N_d$. We find that, roughly, when the number of attackers $N_a/3 \gtrsim N_d$, the empirical harm is much larger than the analytical harm and the population-level model breaks down.

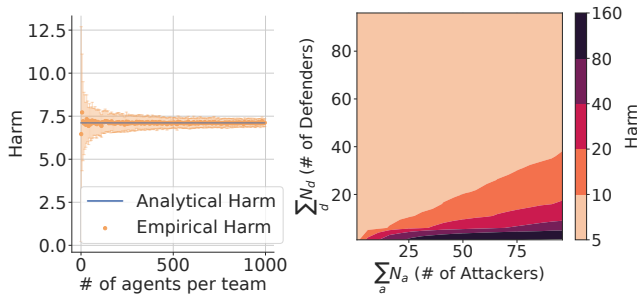


Fig. 4: Influence of a limited number of agents on the theory. **Left:** For a fixed Q_a and the corresponding P_d^* , we estimate the empirical harm across 100 independent runs for the number of agents $\sum_a N_a = \sum_d N_d \in [1, 1000]$. While the mean empirical harm is close to the analytical harm, the variance of the empirical harm decreases as we increase the number of agents. **Right:** We next sweep both number of attackers $\sum_a N_a$ and the number of defenders $\sum_a N_d$. The analytical harm ≈ 7.113 for this Q_a and its P_d^* ; the empirical harm is close to this, roughly up to $\sum_a N_a/3 \gtrsim \sum_d N_d$.

VI. ESTIMATING AN UNKNOWN ATTACKER DISTRIBUTION

We are next interested in understanding scenarios when the attacker distribution Q_a is not known to the defenders and the distribution changes over time. We will change the attacker distribution in two ways: (a) different types of attackers arrive as time progresses, and (b) attackers shift in the shape-space by changing their capabilities. These are both motivated by the setting where an adversary reallocates the composition of the attacker team after observing a few iterations of the interaction. Our strategy will be to estimate the changing attacker distribution $Q_a(t)$ and use this estimate to calculate a new optimal distribution for defenders $P_d^*(t)$ at each time step. Interactions, both successful or not, provide us observations of the attacker types a that exist in the environment, and thereby the distribution $Q_a(t)$.

Our model for how attackers proliferate enables us to estimate their distribution as follows. Let us first assume that Q_a is unknown to the defenders but it is stationary, i.e., it does not change with time. From §III, the expected number of attackers is $m_a(t)$ and it grows as $m_a(t) = m_a(0)e^{\nu_a t}$. We

assume that $m_a(0) = 1$ for attackers a that were sampled from Q_a . If we can estimate $\hat{m}_a(0)$ then we can think of the attackers corresponding to it as sampled from Q_a and obtain an estimate \hat{Q}_a .

Let us arrange all the attackers into a vector $x(t) \in \mathbb{R}^{m_a(t)}$ which will be the state of our filter. We will assume that $x_i \sim N(\mu_i, \sigma_i)$ for $i \leq m_a(t)$ and we receive observations $y_i = cx_i + \xi$ where c is a Boolean that indicates if this specific attacker interacted with the defenders and $\xi \sim N(0, \sigma_\xi^2)$ is Gaussian noise. We can update $\mu_i^+ = \mu_i + k(y_i - c\mu_i)$ and $(\sigma_i^+)^2 = (1 - kc)\sigma_i^2$ using the Kalman gain $k = \sigma_i^2 c / (c^2 \sigma_i^2 + \sigma_\xi^2)$. The growth rate can now be estimated as $\hat{\nu}_i = \log(\mu_i^+ / \mu_i)$. Since there are multiple attackers for each type, we average the estimates

$$\hat{\mu}_a(t) = \frac{\sum_{i=1}^{m_a(t)} \mathbf{1}_{\{\text{type}(x_i)=a\}} \mu_i}{\sum_{i=1}^{m_a(t)} \mathbf{1}_{\{\text{type}(x_i)=a\}}},$$

and similarly for $\hat{\nu}_a$ to get $\hat{Q}_a(t) = \hat{\mu}_a e^{-\hat{\nu}_a t}$. Let us emphasize that the number of attackers $m_a(t)$ (and therefore the dimensionality of the state x of the filter) grows with time but this can be handled in the implementation easily. As written, this filter runs independently for each attacker (and therefore each attacker type) but it is easy to incorporate a known model of the correlations between the growth rates ν_a of different attacker types. Given the estimate of $\hat{Q}_a(t)$, we recalculate the optimal defender distribution $P_d^*(t)$ by minimizing (3) at each instant.

Fig. 5 discusses simulation experiments using an unknown and stationary Q_a using the above filter. At the beginning of each episode, we sample a new set of attackers from Q_a and within every episode $0 \leq t \leq T$, we sample defenders from $P_d^*(t)$ that is calculated using the $\hat{Q}_a(t)$ estimated by the filter. We initialize $\hat{Q}_a(0)$ to be uniform and $P_d^*(0)$ using (3). The episode ends at a random time T when the final attacker is recognized by the defense and the total harm of that episode is the harm incurred until all attackers are recognized. The estimate of \hat{Q}_a is initialized to its final value $\hat{Q}_a(T)$ from the previous episode. In other words, defenders get multiple opportunities to estimate the attacker distribution. *Attacker types* can be different across episodes but the attacker distribution Q_a is the same across episodes. We run each experiment for 100 episodes.

Fig. 5 (top left) shows that the Wasserstein distance between the true Q_a and the estimated \hat{Q}_a decreases with the number of episodes. Due to the stochasticity of the observations, the filter estimates an approximate value \hat{Q}_a which has a higher coefficient of variation κ than that of the true Q_a (seen as shorter spikes in Fig. 5 bottom left). Note that even if the estimation procedure does not recover the true Q_a the corresponding optimal defender distribution $P_d^*(\hat{Q}_a)$ is close to $P_d^*(Q_a)$ in terms of the Wasserstein metric. This has important practical implications: we can obtain near-minimal harm even with incomplete information of the attacker team's constitution for large multi-agent problems (this simulation has 1000 attackers and 1000 defenders). The fundamental reason for this is cross-reactivity $f_{d,a}$; a given defender type

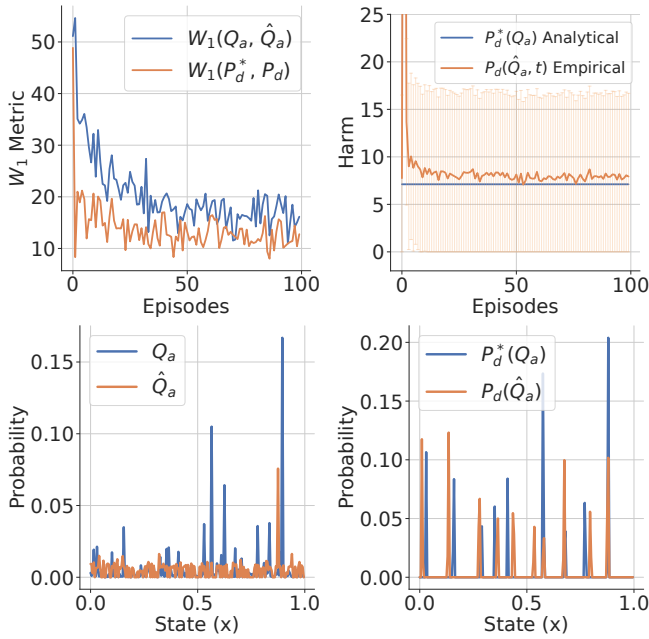


Fig. 5: Estimating an unknown and stationary attacker distribution. **Top:** We plot the W_1 metric between the ground truths Q_a, P_d^* against estimates \hat{Q}_a, P_d over episodes. On the right we compare P_d^* analytical harm and empirical harms' means and standard deviations as the defenders gain a better estimation of Q_a . **Bottom:** We show the final \hat{Q}_a estimated at the end of 100 episodes (orange) against the actual Q_a (blue) in the left plot. On the right, we have ground truth $P_d^*(Q_a)$ and estimated $P_d(\hat{Q}_a)$.

can counter, even if sub-optimally, many other attacker types.

We derived the above filter for a stationary Q_a . If the attacker distribution is non-stationary and evolves with time, we can still use the same expressions to estimate $\hat{Q}_a(t)$. This will be sub-optimal but if the timescale of the evolution of Q_a is much slower than the growth rates ν_a and ν'_a (which determine how quickly the defenders interact and thereby recognize the attackers), then we can expect the estimate $\hat{Q}_a(t)$ to converge faster than the rate of change of $Q_a(t)$. We will tacitly make this assumption.

Fig. 6 discusses simulation experiments with a non-stationary Q_a with the same setup as that of Fig. 5. We shift the attacker distribution as $Q_{a+k} = Q_a$, i.e., after the k^{th} episode, the probability of observing attacker $a+k$ is Q_a . We can implement this case easily by noticing that the interval $[0,1]$ is isomorphic to $[0, 2\pi]$. This experiment shows how cross-reactivity allows the defenders to both track and counter different types of attacker distributions even if the estimation is not perfect in capturing the large spikes in Q_a . The broad trends are similar to those of Fig. 5. But it is interesting to note that the variance of the harm is much smaller in this case than in Fig. 5 (top right); this is perhaps because even if the estimate $\hat{Q}_a(t)$ and the corresponding $P_d^*(\hat{Q}_a(t))$ are inaccurate, the true attacker distribution changes in the next episode. This suggests that even for non-stationary problems, it is possible to achieve near-optimal harm; cross-reactivity is the key ingredient of the model that makes this possible.

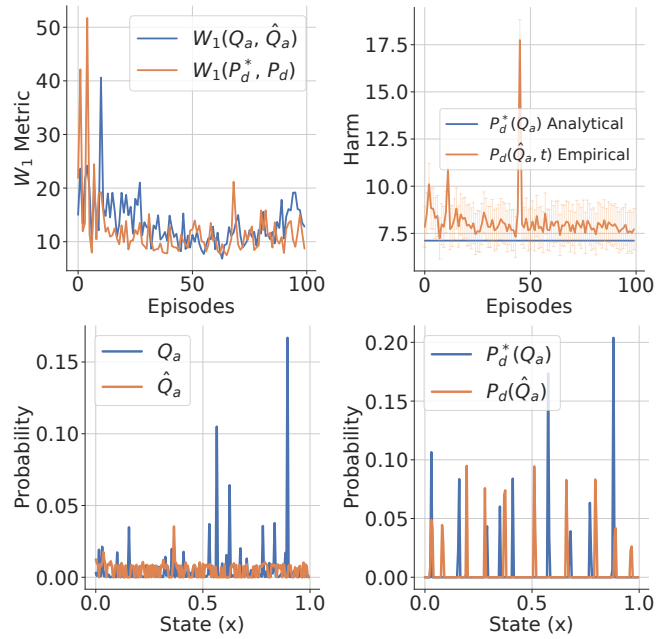


Fig. 6: Estimating an unknown and changing attacker distribution. **Top:** Even when the attacker distribution is changing with time, the filter can track this distribution (the error is slightly higher than the one in Fig. 5 top left), and both the defender distribution and the harm incurred are close to their optimal values at the end of the experiment. **Bottom:** The estimate \hat{Q}_a now matches the diversity of the true attacker distribution (bottom left) but does not estimate the probabilities of the spikes as accurately. This causes the estimated $P_d^*(\hat{Q}_a(t))$ to be slightly different than the true $P_d^*(Q_a(t))$ (bottom right).

VII. COMPETITION BETWEEN DEFENDERS LEADS TO OPTIMAL RESOURCE ALLOCATION

The optimal defender distributions P_d^* so far were calculated in a centralized fashion. We next discuss how the optimal defender distribution can also emerge from a decentralized computation. The key idea is to exploit cross-reactivity between the defenders, i.e., the fact that multiple defenders can tackle the same attacker and set up competition among the defenders to earn the reward of successfully recognizing an attacker. Biology does things in a similar way: receptors that successfully recognize antigens proliferate at the cost of other receptors [32]. Let the number of defenders of a particular type be N_d . We can set

$$\frac{dN_d}{dt} = N_d \left[\sum_a Q_a \varphi \left(\sum_{d'} N_{d'} f_{d',a} \right) f_{d,a} - c \right]. \quad (5)$$

Here, the constant c is the rate at which defenders d are decommissioned (this would be the death rate in biology). In the first term, the total interaction of defender d with different attackers $\sum_a Q_a f_{d,a}$ is weighted by some function $\varphi(\cdot)$ which is a decreasing function of its argument. The quantity $\sum_{d'} N_{d'} f_{d',a}$ determines how many other defenders can tackle a . If this is large, then the incremental utility of having the specific defender d diminishes, and therefore its growth rate \dot{N}_d should be smaller.

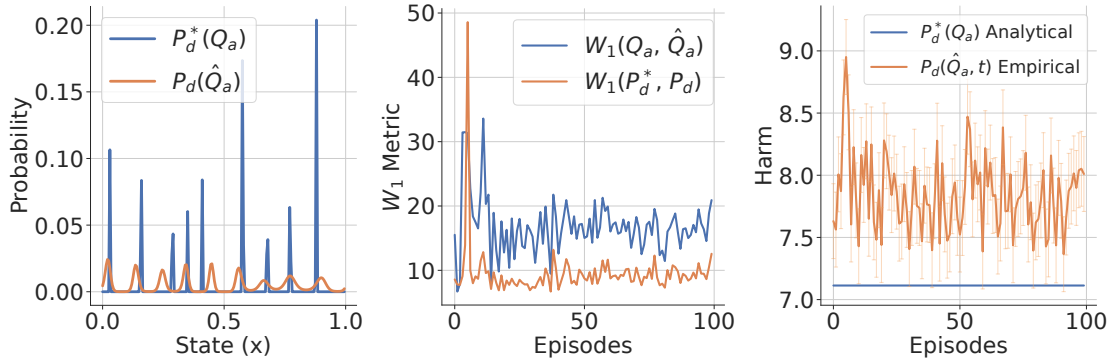


Fig. 7: Convergence to near-optimal harm with competition dynamics. For the same setting as that of Fig. 5, we run the dynamics in (5) using the estimate $\hat{Q}_a(t)$ calculated using the Kalman filter to induce the defender distribution $P_d(t)$ (instead of calculating it by minimizing the harm in (3) as done in Fig. 5). We run the population dynamics for 10^6 iterations within each episode. The defender distribution P_d (orange, left) is close to the optimal distribution P_d^* for Q_a but it is a bit smoother and therefore sub-optimal (higher harm in the right panel).

A short calculation, which follows Appendix F of [1], gives that the stable fixed point N_d^* of (5) gives the probability distribution $P_d^* = N_d^* / (\sum_{d'} N_{d'}^*)$ for the harm to be minimized. For this to happen, we need $\varphi(\tilde{N}_a) = -b' d\bar{F} / dm |_{m=(\tilde{N}_a/N_{st})}$, where $\tilde{N}_a = \sum_d N_d^* f_{d,a}$ and N_{st} is the total number of defenders at the fixed point. The fixed point is found by setting $\dot{N}_d = 0$. For the nontrivial solution where $N_d > 0$, notice that substituting $\varphi(\tilde{N}_a)$ into (5) gives $\sum_a Q_a \bar{F}'(\tilde{P}_a) f_{d,a} = -b'c$ which is equivalent to the optimality condition for (3).

Fig. 7 shows an experiment with this competition dynamics for a stationary attacker distribution Q_a . The harm converges to the optimal harm for a centralized computation of P_d^* . We can also use the estimated attacker distribution \hat{Q}_a in place of the true distribution Q_a in (5) in situations where it is unknown to the defenders. It is interesting to note that the competition dynamics gives a P_d that does not have the sharp spikes like P_d^* (left). And this is why the empirical harm is slightly higher than the optimal harm. We know from Fig. 2 that there is a tradeoff between the diversity of the defender types (many types for a smooth distribution to few types for a spiked distribution) and harm (lower harm for the smooth distribution and higher harm for same recognition probability for the latter). This experiment suggests that competition dynamics can lead to near-optimal policies for multi-agent interaction problems.

VIII. COMPARISON WITH REINFORCEMENT LEARNED POLICIES

We next use a reinforcement learning algorithm called soft actor-critic (SAC) [33] to minimize the empirical harm (2) and learn a policy for the team of defenders. Our goal is to compare the learned defender distribution from RL to the competition dynamics in §VII and the optimal defender distribution.

At the beginning of each episode, we initialize the defender distribution P_d to a uniform distribution and sample N_d defenders from it. We sample N_a attackers from a Q_a that is fixed across episodes. At each time-step, defenders optimize the parameters θ of a neural network to learn a control policy which gives a discrete control $[-\Delta, 0, \Delta] \ni \bar{u} = \pi_\theta(d, \hat{Q}_a)$

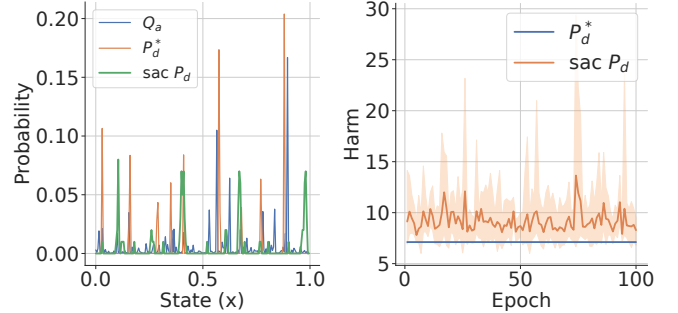


Fig. 8: Defender distribution P_d learned by SAC at the end of an episode after competing for interactions with attackers sampled from Q_a (blue, the optimal P_d^* is in orange). We sampled $\sum_d N_d = 100$ agents from a uniform distribution shift states to perform recognition. On the right we compare the test harm of the defender distribution P_d learned by SAC over training epochs to the optimal harm.

that reallocates a defender agent from type d to type $d + \bar{u}$; we set $\Delta = 0.005$. Weights θ are shared by all defender agents. Analogous to the changing attacker distribution in §VI, this setting alludes to the defenders reallocating their resources using information from the interactions. We can now simulate the attacker dynamics (at each time-step, attackers proliferate at rate $\nu_a m_a(t)$ and interactions increase with rate is $\nu_a' \lambda_a(t)$) to obtain one rollout. The return of this rollout is $R = -\sum_a \dot{m}_a(t)$ which is the rate of proliferation of the attackers; note that the number of attackers that are not recognized grows as $\dot{m}_a(t) = \nu_a m_a$ so minimizing this rate effectively encourages the policy to recognize attackers. This quantity is also incidentally what we calculated while building the filter in §VI to estimate \hat{Q}_a . The RL policy should be compared to the competition dynamics in §VII because defenders compete for interactions with the attackers to earn the reward of successful recognition. Note that at the end of the episode, we can also calculate the effective defender distribution obtained by the SAC policy $P_d = N_d / \sum_{d'} N_{d'}$.

In Fig. 8, the SAC policy moves defenders, starting from a uniform distribution, such that they form a peaked distribution to compete for interactions. The distribution P_d at the end

of the episode is not the same as the optimal distribution P_d^* and it achieves higher harm (about 10) than the one learned from the competition dynamics in Fig. 7 (about 8).

IX. CONCLUSION

In this work, we develop a model to understand what an optimal defensive repertoire looks like. The key property of this model is cross-reactivity which enables defender agents of a given type to recognize attackers, of a few different types. This allows the defender distribution to be supported on a discrete set, even if the shape-space, i.e., the number of different types of agents, is very large. Cross-reactivity is also fundamentally responsible for the defender team to be able to estimate an unknown and evolving attacker distribution.

We saw how this model points to a number of guiding principles for the design of multi-agent systems across many different scales and problem settings, e.g., the immune system where the population-level dynamics of the attackers and defenders that was used to formulate the model, to various experimental settings where we evaluated the model with a finite number of agents, to competition dynamics that allows effective decentralized control policies and reinforcement learning such controllers.

In the future, we hope to seek parallels of these ideas with specific strategies and the evolution of these strategies in multi-agent games such as soccer or basketball. There are certain similarities: teams like to be constituted of players that can cover the opponent team's repertoire of speed, skill, size and strength. This is an example of "zone" defense and a generalist strategy; it prevents a specific opponent from maximizing their capabilities. Man-to-man strategies, which would be akin to a small cross-reactivity bandwidth in our model, work well when the opponent distribution is known well, but they are not robust to changes or incorrect estimates of the opponent distribution. The key difference in these problems to those explored here is that these problems are highly dynamic games with evolving strategies, objectives, and consequently dynamic equilibria. Our population-level, steady-state model is not ideal for understanding such problems.

REFERENCES

- [1] A. Mayer, V. Balasubramanian, T. Mora, and A. M. Walczak, "How a well-adapted immune system is organized," *PNAS*, vol. 112, no. 19, pp. 5950–5955, 2015.
- [2] S. Karaman and E. Frazzoli, "Incremental sampling-based algorithms for a class of pursuit-evasion games," vol. 68, pp. 71–87, 01 2010.
- [3] R. Isaacs, *Differential Games I*. RAND Corporation, 1954.
- [4] T. Chung, G. Hollinger, and V. Isler, "Search and pursuit-evasion in mobile robotics," *Auton. Robots*, vol. 31, 11 2011.
- [5] C. Robin and S. Lacroix, "Multi-robot Target Detection and Tracking: Taxonomy and Survey," *Autonomous Robots*, vol. 40, no. 4, pp. 729–760, 2016.
- [6] V. Kumar, D. Rus, and S. Singh, "Robot and sensor networks for first responders," *IEEE Pervasive Computing*, vol. 3, no. 4, p. 24–33, 2004.
- [7] M. Dunbabin and L. Marques, "Robots for environmental monitoring: Significant advancements and applications," *RAM*, vol. 19, no. 1, pp. 24–39, 2012.
- [8] A. R. Hilal, "An intelligent sensor management framework for pervasive surveillance," 2013.
- [9] M. Tan, "Multi-agent reinforcement learning: Independent vs. cooperative agents," in *ICML*, pp. 330–337, 1993.
- [10] R. Lowe, Y. Wu, A. Tamar, J. Harb, P. Abbeel, and I. Mordatch, "Multi-agent actor-critic for mixed cooperative-competitive environments." arXiv 1706.02275, 2020.
- [11] S. Li, J. K. Gupta, P. Morales, R. Allen, and M. J. Kochenderfer, "Deep implicit coordination graphs for multi-agent reinforcement learning." arXiv 2006.11438, 2021.
- [12] K. Son, D. Kim, W. J. Kang, D. E. Hostallero, and Y. Yi, "Qtran: Learning to factorize with transformation for cooperative multi-agent reinforcement learning." arXiv 1905.05408, 2019.
- [13] B. Baker, I. Kanitscheider, T. Markov, Y. Wu, G. Powell, B. McGrew, and I. Mordatch, "Emergent tool use from multi-agent autocurricula." arXiv 1909.07528, 2020.
- [14] Q. Long, Z. Zhou, A. Gupta, F. Fang, Y. Wu, and X. Wang, "Evolutionary population curriculum for scaling multi-agent reinforcement learning." arXiv 2003.10423, 2020.
- [15] C. D. Hsu, H. Jeong, G. J. Pappas, and P. Chaudhari, "Scalable reinforcement learning policies for multi-agent control," in *IROS*, pp. 4785–4791, 2020.
- [16] M. A. Hsieh, Á. M. Halász, S. Berman, and V. R. Kumar, "Biologically inspired redistribution of a swarm of robots among multiple sites," *Swarm Intelligence*, vol. 2, pp. 121–141, 2008.
- [17] M. M. Zavlanos, H. G. Tanner, A. Jadbabaie, and G. J. Pappas, "Hybrid control for connectivity preserving flocking," *TAC*, vol. 54, no. 12, pp. 2869–2875, 2009.
- [18] A. Mitra, H. Hassani, and G. Pappas, "Exploiting heterogeneity in robust federated best-arm identification," 2021.
- [19] T. Wang, T. Gupta, A. Mahajan, B. Peng, S. Whiteson, and C. Zhang, "Rode: Learning roles to decompose multi-agent tasks." arXiv 2010.01523, 2020.
- [20] T. Salam and M. A. Hsieh, "Heterogeneous robot teams for modeling and prediction of multiscale environmental processes." arXiv 2103.10383, 2021.
- [21] D. Shishika, J. Paulos, M. R. Dorothy, M. Ani Hsieh, and V. Kumar, "Team composition for perimeter defense with patrollers and defenders," in *CDC*, pp. 7325–7332, 2019.
- [22] K. Szwaykowska, I. B. Schwartz, L. Mier-y Teran Romero, C. R. Heckman, D. Mox, and M. A. Hsieh, "Collective motion patterns of swarms with delay coupling: Theory and experiment," *Phys. Rev. E*, vol. 93, p. 032307, 2016.
- [23] V. Edwards, P. Rezeck, L. Chaimowicz, and M. A. Hsieh, "Segregation of Heterogeneous Robotics Swarms via Convex Optimization," *Dynamic Systems and Control Conference*, 10 2016.
- [24] L. Chaimowicz, A. Cowley, D. Gomez-Ibanez, B. Grocholsky, M. A. Hsieh, H. Hsu, J. F. Keller, V. Kumar, R. Swaminathan, and C. J. Taylor, "Deploying air-ground multi-robot teams in urban environments," in *Multi-Robot Systems. From Swarms to Intelligent Automata Volume III*, pp. 223–234, 2005.
- [25] B. Grocholsky, J. Keller, V. Kumar, and G. Pappas, "Cooperative air and ground surveillance," *RAM*, vol. 13, no. 3, pp. 16–25, 2006.
- [26] M. Bettini, A. Shankar, and A. Prorok, "Heterogeneous multi-robot reinforcement learning," 2023.
- [27] H. Ravichandar, K. Shaw, and S. Chernova, "Strata: A unified framework for task assignments in large teams of heterogeneous agents," 2019.
- [28] A. S. Perelson and G. F. Oster, "Theoretical studies of clonal selection: Minimal antibody repertoire size and reliability of self-non-self discrimination," *Journal of Theoretical Biology*, vol. 81, no. 4, pp. 645–670, 1979.
- [29] J. G. Smith, "The information capacity of amplitude-and variance-constrained scalar Gaussian channels," *Information and control*, vol. 18, no. 3, pp. 203–219, 1971.
- [30] J. O. Berger, J. M. Bernardo, and D. Sun, "The formal definition of reference priors," *The Annals of Statistics*, vol. 37, no. 2, pp. 905–938, 2009.
- [31] F. Santambrogio, "Optimal transport for applied mathematicians," *Birkhäuser, NY*, vol. 55, no. 58-63, p. 94, 2015.
- [32] R. J. De Boer and A. S. Perelson, "T cell repertoires and competitive exclusion," *Journal of Theoretical Biology*, vol. 169, no. 4, pp. 375–390, 1994.
- [33] T. Haarnoja, A. Zhou, P. Abbeel, and S. Levine, "Soft actor-critic: Off-policy maximum entropy deep reinforcement learning with a stochastic actor," 2018.